Contents lists available at ScienceDirect

Heliyon

Research article

The use of complex formation manner for spectrophotometric analysis of gatifloxacin drug based on Co(II), Ni(II) and La(III) ions

Mona M. Mostafa [a], Zeinab H. Abd El-Wahab [b,*], Aida A. Salman [b], W.M. Abdelbaset [a]

[a] National Organization for Drug Control & Research (NODCAR), Agouza, Dokki, Cairo, Egypt
[b] Chemistry Department, Faculty of Science (Girl's), Al-Azhar University, Youssif Abbas St., Nasr-City, P.O. Box 11754, Cairo, Egypt

ARTICLE INFO

ABSTRACT

Herein, a simple and accurate spectrophotometric method was developed to detect gatifloxacin (HGAT) in a pure and ophthalmic formulation. The method depends on complexation of HGAT with Co (II), Ni (II) and La(III) ions in ethanol medium at room temperature. The experimental conditions have been investigated to reach optimum conditions for HGAT-metal ions interaction, including detection of a suitable wavelength, medium pH, reaction time and reactants concentration. Moreover, the composition of these complexes in addition to their stability constants were also investigated and the result indicated that the molar ratio of HGAT: Metal ion is 1:1 for Ni (II) and La(III) ions and 1:2 for Co (II) ion. Beer's law plots were obeyed in the concentration ranges 18.77–150.16, 18.77–131.39 and 18.77–112.62 (μg mL^{-1}) for Co(II), Ni(II) and La(III) ions interaction, respectively. The apparent molar absorptivity, Sandell's sensitivity, standard deviation, detection and quantification limits were calculated. The proposed method was successfully applied for the determination of HGAT in the bulk and ophthalmic formulation. The obtained results were compared statistically with other published methods and the results were in good agreement with those obtained by reported methods.

1. Introduction

Gatifloxacin (HGAT), Figure 1 is an important member of fluoroquinolone family known as [1-cyclopropyl-6-fluoro-1,4-dihydro-8-methoxy-7-(3-methyl piperazine-1-yl)-4-oxo-3-quinoline carboxylic acid] and has been widely used to treat the infections in human medicine caused by Gram-positive and Gram-negative bacteria [1, 2]. Although in reviewing the literature, no official technique has yet been reported for HGAT evaluation in its bulk and pharmaceutical formulation [3, 4], there are a lot of analytical methods have been reported by many researchers describe HGAT determination including UV-vis spectrophotometry, atomic absorption spectrophotometry, spectrofluorometry, liquid chromatography, high-performance liquid chromatography, liquid chromatography-mass spectrometry, fluorescence methods, capillary electrophoresis and flow injection analysis [5, 6, 7, 8, 9, 10]. Generally, UV-vis spectrophotometric determination is the most widely used method for drugs determination in their dosage forms due to its simplicity, low cost and wide availability in laboratories [11]. Based on the literature review, various methods have been reported for HGAT determination using UV-vis spectrophotometry [12, 13, 14, 15] but there

is few reports describe HGAT determination via its interaction with the metal ions in solution [16].

For that reason, our study aimed to develop and validate a novel simple and sensitive spectrophotometric method for HGAT determination in its bulk and ophthalmic formulation (Tymer sample) through its interaction with Co(II), Ni(II) and La(III) ions in solution. The experiments were also performed to investigate the stability constant of HGAT - metal ions interaction. Also, the proposed method was compared with other published methods to evaluate its use in routine assay for its pharmaceutical dosage forms.

2. Experimental section

2.1. Chemicals and pharmaceutical formulations

HGAT drug has a potency of 99.20 % (Batch No. JT20151102) was kindly supplied by Delta Grand Pharma. HGAT in its ophthalmic formulation as Tymer sample; 5 mL (0.3% sterile ophthalmic solution) labeled to be 3 mg HGAT/1mL (Batch No. WC0061) produced by Jamjoom Pharmaceuticals Co., Jeddah, Saudi Arabia. Cobalt (II) Chloride hexahydrate (Merck), nickel (II) chloride hexahydrate (Aldrich) and

lanthanum (III) Chloride hexahydrate (Fluka). Hydrochloric, nitric and sulphuric acids in addition to lithium hydroxide monohydrate (EL-Nasr Chemical Co. Egypt). Ethanol 99.99 % (ADWIC). Disodium salt of ethylenediaminetetraacetic acid, Na_2-EDTA (Prolabo); ammonia solution 25% (Abco Chemie ENG. LTD); xylenol orange were analytical grade and were used as supplied. De-ionized water was used in the preparation of the required solutions.

2.2. Apparatus

2.2.1. UV–visible absorption spectral measurements

For the absorbance measurements, UV-Vis spectrophotometer, model UNICAM equipped with quartz cell of 1 cm optical length in the range 200–800 nm was used. The instrument recorded the signal of absorbance (A) vs. wavelength (λ/nm).

2.2.2. Atomic absorption spectrometer measurements

The atomic absorption measurements to determine the concentration of metal ions/drug under study were carried out using a SOLAAR atomic absorption series spectrometer.

2.2.3. The pH measurement

The pH value of the prepared solutions was monitored using JENWAY 3450 pH and conductivity Meter. The pH meter was calibrated with standard buffer solutions (pH 4.0 and 7.0) before the pH measurements.

2.3. Preparation of stock solution

2.3.1. Cobalt chloride solution

A weight of 0.2379 g of cobalt chloride hexahydrate, $CoCl_2.6H_2O$ was dissolved in a small amount of ethanol then completed to 100 ml in a measuring flask to obtain $1 \times 10^{-2} ML^{-1}$ solution. The concentration of $CoCl_2.6H_2O$ solution was checked by SOLAAR atomic absorption series spectrometer.

2.3.2. Nickel chloride solution

A weight of 0.2377 g of nickel chloride hexahydrate, $NiCl_2.6H_2O$ was dissolved in a small amount of ethanol then completed to 100 ml in a measuring flask to obtain $1 \times 10^{-2} ML^{-1}$ solution. The concentration of $NiCl_2.6H_2O$ solution was checked by SOLAAR atomic absorption series spectrometer.

2.3.3. Lanthanum chloride solution

A weight of 0.3534 g of lanthanum chloride hexahydrate, $LaCl_3.6H_2O$ was dissolved in a small amount of ethanol then completed to 100 mL in a measuring flask to obtain an approximate $1 \times 10^{-2} ML^{-1}$ solution. The concentration of $LaCl_3.6H_2O$ solution was checked complexometrically using xylenol orange as an indicator [17, 18].

2.3.4. Lithium hydroxide solution

An aqueous solution of lithium hydroxide monohydrate 1×10^{-2} ML^{-1} was prepared by appropriate dilution of a standard concentrated solution (1.0 M) with deionized water in a volumetric flask.

2.3.5. Hydrochloric acid solution

An aqueous solution of hydrochloric acid ($1 \times 10^{-2} ML^{-1}$) was prepared by appropriate dilution of the standard concentrated solution (1.0 M) with deionized water in a volumetric flask.

2.3.6. Working solution of bulk and ophthalmic sample of gatifloxacin

For a bulk sample of HGAT in its pure powder form, a stock solution of $1 \times 10^{-2} ML^{-1}$ is prepared by dissolving 0.3754 g of HGAT in the least amount of ethanol then completed to 100 mL in a measuring flask. The required working solutions were freshly prepared by accurate dilution of the stock solution as needed. For the ophthalmic sample, the content of two containers was mixed well by shaking then an aliquot of 1, 2 and 3

mL of the resulting solution were transferred separately to a 100 mL volumetric flask and the volume was completed to the mark with bidistilled water to obtain a sample solution containing 30, 60 and 90 µg/mL of HGAT. After that, aliquots covering the working concentration ranges were analyzed as described under the construction of the calibration curve. The concentration of HGAT was determined using, either the calibration curves or the corresponding regression equation.

2.4. Gatifloxacin - metal ions interaction and optimized conditions

To establish the most favorable conditions for HGAT - metal ions interaction, different experimental conditions are carefully studied and optimized such as a selection of a suitable wavelength for measurement, pH of the medium, reaction time and concentration of the reactants. Moreover, for optimization of the reaction conditions, the studied parameter was varied while the others were kept constant.

2.4.1. Selection of analytical wavelength

For the selection of the analytical wavelength of HGAT, the working test solution of HGAT ($1 \times 10^{-2} ML^{-1}$) was scanned between 200 to 900 nm at room temperature using a UV–Vis spectrophotometer against ethanol as blank. Additionally, the analytical wavelength for HGAT - metal ions interaction can be detected as; in a clean calibrated 5 mL volumetric flask, 1 mL of $1 \times 10^{-2} ML^{-1}$ of $CoCl_2.6H_2O$, $NiCl_2.6H_2O$ and $LaCl_3.6H_2O$ solution, separately added to 1 mL of $1 \times 10^{-2} ML^{-1}$ of HGAT solution, then each solution was made up to the mark with ethanol and mixed thoroughly by shaking. After that, a portion of each solution was carefully transferred into a 1 cm quartz cell and the absorption was recorded at room temperature over a spectral range of 200–900 nm by scanning on a UV–Vis spectrophotometer against ethanol as blank [19]. Finally, the wavelength with the maximum absorbance, λ_{max}, namely was determined.

2.4.2. pH value of the medium

For the pH- optimization experiment, 1.0 M HCl/LiOH.H_2O was used and all pH values were measured by a pH meter at room temperature till turbidity or formation of a precipitate was observed. Typically, in a clean calibrated 5 ml flask, 1 mL of $1 \times 10^{-2} ML^{-1}$ of $CoCl_2.6H_2O$, $NiCl_2.6H_2O$ and $LaCl_3.6H_2O$ solution, separately added to 1 mL of $1 \times 10^{-2} ML^{-1}$ of HGAT solution, then the pH value of the solution was adjusted to the required value. After that, the absorption of each solution was recorded at room temperature at a specialized wavelength against ethanol as a blank. The optimum pH value was determined [20].

2.4.3. Reaction time

In order to realize the best condition for HGAT - metal ions interaction, the reaction time of such interaction was determined. The experiment was carried out by recording the absorbance of the solution at different time intervals under the optimum conditions stated before [21].

2.5. Composition of the metal complexes in solution

2.5.1. Job's continuous variation method

Series of solutions were then prepared in 10 mL calibrated measuring flasks containing different volumes of the metal ions solutions of
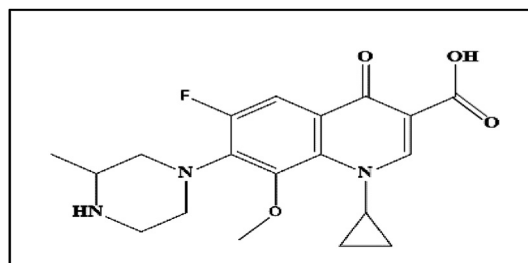

Figure 1. The skeleton structure of gatifloxacin, HGAT.

Table 1. Job's method design.

Run NO.	Composition of the reaction mixture[a]				Absorbance measurements		
	[M] (mL)	[HGAT] (mL)	[M] + [HGAT]	$\frac{[HGAT]}{[(M) + (HGAT)]}$	Co(II) - [HGAT] interaction	Ni(II) - [HGAT] interaction	La(III) - [HGAT] interaction
1	0.95	0.05	1.00	0.05	0.25	0.18	0.35
2	0.90	0.10	1.00	0.10	0.34	0.26	0.43
3	0.80	0.20	1.00	0.20	0.52	0.44	0.60
4	0.70	0.30	1.00	0.30	0.68	0.60	0.76
5	0.60	0.40	1.00	0.40	0.85	0.77	0.93
6	0.50	0.50	1.00	0.50	1.02	0.90	1.05
7	0.40	0.60	1.00	0.60	1.18	0.80	0.92
8	0.34	0.66	1.00	0.66	1.25	0.71	0.82
9	0.30	0.70	1.00	0.70	1.20	0.65	0.76
10	0.20	0.80	1.00	0.80	0.91	0.48	0.57
11	0.10	0.90	1.00	0.90	0.53	0.30	0.37
12	0.05	0.95	1.00	0.95	0.30	0.20	0.25

[M] is represent concentration of metal ions; Co(II), Ni(II) or La(III).

$\frac{[HGAT]}{[(M) + (HGAT)]}$ is represent mole fraction of HGAT/(metal ion + HGAT).

[a] [HGAT] is represent concentration of HGAT.

CoCl$_2$.6H$_2$O, NiCl$_2$.6H$_2$O and LaCl$_3$.6H$_2$O salts (1×10^{-2} ML^{-1}) and HGAT drug solution (1×10^{-2} ML^{-1}) while keeping the total volume the same (1 mL) in each solution. Such series are characterized by the total number of moles are constant but the mole ratio of components varies systematically. After that, the pH was maintained at optimum value for each metal ion and the volume was adjusted to 10 mL then the absorbance of each resulting solution was then measured at room temperature and the specified wavelength (λ_{max}) previously determined against the blank solution. The measured absorbance values were plotted as a function of mole fraction of HGAT [22]. Job's method design was given in Table 1.

2.5.2. Molar ratio method

A series of solutions were prepared in which the total concentration of the metal ion is held constant while HGAT concentration is varied under similar conditions. The absorbance of each resulting solution was then measured at room temperature at its optimum pH value and the specified

wavelength (λ_{max}) was previously determined against the blank solution. After that, the absorbance values were plotted as a function of mole fraction of [HGAT]/[metal ion] [23]. The molar ratio's method design was given in Table 2.

2.6. Assay of gatifloxacin and calibration graph construction

For the analysis of HGAT in its bulk powder, a standard solution for HGAT drug (1×10^{-3} ML^{-1}) was used under the studied optimum conditions. Typically, to eight sets of 10 mL volumetric flasks, 1.0 mL of each metal ion; Co(II), Ni(II) and La(III) ions (1×10^{-2} ML^{-1}) was transferred, then aliquots of the working standard solution for HGAT (0.5, 1.0, 1.5, 2.0, 2.5, 3.0, 3.5 and 4.0 mL) were pipetted each into its corresponding set then the total volume completed up to 10 mL with ethanol under the studied optimum conditions. After that, the absorbance at the specified λ_{max} for each metal ion was measured at room temperature against a blank solution similarly prepared but omitting the

Table 2. Molar ratio's method design.

Run NO.	Composition of the reaction mixture[a]			Absorbance measurements		
	[HGAT] (mL)	[M] (mL)	$\frac{[HGAT]}{[M]}$	Co(II) - [HGAT] interaction	Ni(II) - [HGAT] interaction	La(III) - [HGAT] interaction
1	0.20	1.00	0.20	0.30	0.60	0.50
2	0.40	1.00	0.40	0.40	0.70	0.60
3	0.60	1.00	0.60	0.50	0.81	0.71
4	0.80	1.00	0.80	0.60	0.92	0.82
5	1.00	1.00	1.00	0.70	1.00	0.90
6	1.20	1.00	1.20	0.80	1.00	0.90
7	1.40	1.00	1.40	0.90	1.00	0.90
8	1.60	1.00	1.60	0.98	1.00	0.90
9	1.80	1.00	1.80	1.05	1.00	0.90
10	2.00	1.00	2.00	1.10	1.00	0.90
11	2.20	1.00	2.20	1.10	1.00	0.90
12	2.40	1.00	2.40	1.10	1.00	0.90
13	2.60	1.00	2.60	1.10	1.00	0.90
14	2.80	1.00	2.80	1.10	1.00	0.90
15	3.00	1.00	3.00	1.10	1.00	0.90

Ni(II) or La(III) and $\frac{[HGAT]}{[M]}$ is represent mole fraction of HGAT/metal ion.

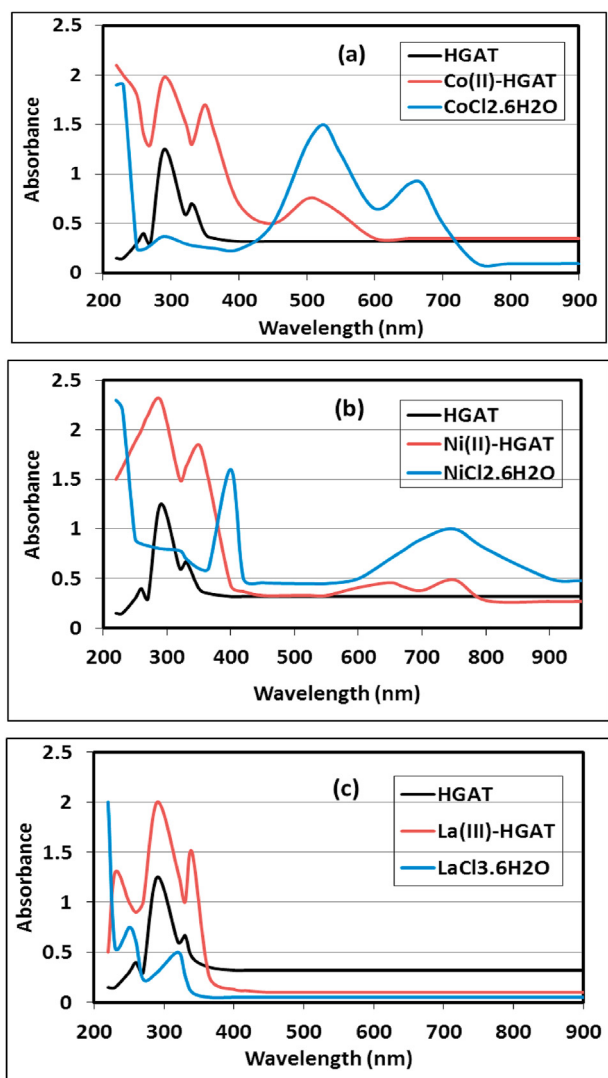[a] [HGAT] is represent concentration of HGAT; [M] is represent concentration of metal ions, Co(II).

Figure 2. Electronic absorption spectra for free HGAT and HGAT – metal ions interaction in solution: (a) Co(II)-HGAT interaction, (b) Ni(II)-HGAT interaction and (c) La(III)-HGAT interaction.

HGAT and plotted against the concentration of HGAT [24]. The measurement for each run was performed five times and the mean value was recorded.

2.7. Estimation of pharmaceutical form as ophthalmic formulation

The proposed spectrophotometric method was extended for the determination of the drug content in an ophthalmic formulation as a
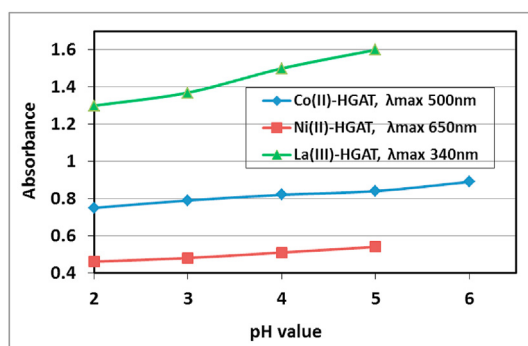

Figure 3. Effect of pH on the absorption value of HGAT-metal ions interaction.

Tymer sample. As described in the experimental part, three different concentration; 30, 60 and 90 μg/mL were used and applying the general procedure in the study. The measurements were performed five times for each concentration within the linear range of the investigated drug and the mean value was recorded.

3. Results and discussion

The main purpose of this work is the determination of gatifloxacin in pure form and in pharmaceutical formulation based on its interaction with Co(II), Ni(II) and La(Ill) ions in solution. HGAT, Figure 1 has the molecular formula ($C_{19}H_{22}FN_3O_4$), the molar mass of 375.394 g/mol and bicyclic ring structure which is a quinoline skeleton having variable functional groups at different positions make it acts as a polydentate ligand [25].

3.1. Spectral characteristics

The initial detection for the affinity of HGAT towards Co(II), Ni(II) and La(Ill) ions was done through UV–Vis spectrophotometric
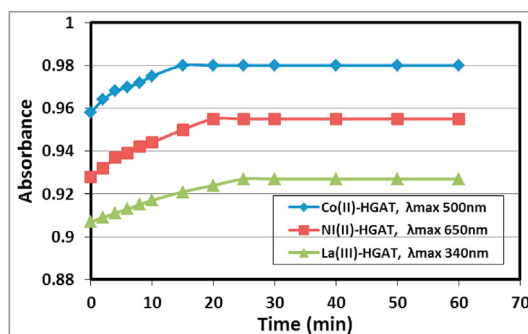

Figure 4. Effect of time on the absorption value of HGAT – metal ions interaction.

Table 3. UV–visible spectrophotometric measurements of pure HGAT and HGAT - metal ions interaction.

Compounds under study	UV–visible spectrophotometric measurements											
	First band			Second band			Third band			Fourth band		
	λ (nm)	Abs	ε	λ (nm)	Abs	ε	λ (nm)	Abs	ε	λ (nm)	Abs	ε
HGAT	260	0.40	40	290	1.25	125	330	0.67	67	–		
HGAT- Co(II) interaction	290	1.98	198	350	1.70	170	500	0.75	75	–		
HGAT- Ni(II) interaction	290	2.30	230	350	1.85	185	650	0.46	46	750	0.49	49
HGAT- La(III) interaction	230	1.30	130	290	2.00	200	340	1.50	150	–		

ε is the molar absorptivity (Lmol^{-1}cm^{-1}) calculated according to Lambert–Beer law, ($A = \varepsilon bc$).{A = absorbance (no units); C = concentration of absorbing species (mol/L) and b = path length (1cm)}.

measurements and comparing the spectrum nature of free HGAT with the spectra of the metal complexes resulted from HGAT - metal ions interaction as shown in Figure 2(a-c). The absorption spectrum of free HGAT in ethanol exhibits three absorption bands in the ultra-violet region at the range of 200–400 nm. The first one is a medium intensity band at 260 nm, the second peak is an intense band at 290 nm while the third one is a medium intensity band at 330 nm. The peaks at 260 and 290 nm attributed to π–π^* electronic transitions of the phenyl, piperazine and pyridone moieties while the peak at 330 nm accounted for n–π^*electronic transitions of the two C=O groups for both the carboxylate and carbonyl groups [26, 27].

Upon interaction of HGAT drug with Co(II), Ni(II) and La(Ill) ions, Figure 2(a-c) respectively, as explained in the experimental part, it was found that the spectra have some bathochromic or hypochromic shift of the absorption bands with different absorbance, in addition, to generate new bands in the visible region at 500–900 nm. For a complete comparison, the spectra of the studied metal chloride salts are also included in Figure 2(a-c). Moreover, the molar absorption coefficient for the complexed HGAT is higher than the value corresponding to free HGAT. All these observations were tabulated in Table 3 and have been attributed to the coordination of HGAT to the metal ions under study [28].

3.2. Effect of pH

The effect of pH change on the absorbance of HGAT - metal ions interaction was studied over the pH range of 2.0–6.0 at room temperature and optimum wavelength as given in Figure 3. Analysis of Figure 3 explains that the absorbance increased with increasing pH value. Moreover, the optimum pH 6.0 was observed for Co(II) - [HGAT] interaction with an absorbance equal to 0.89 while for both Ni(II) - [HGAT] and La(III) - [HGAT] interaction, the optimum pH 5.0 was detected with an absorbance equal to 0.53 and 1.60, respectively. Above these values, a precipitate was observed. Based on the obtained results, the optimum pH value that favors HGAT-metal ions interaction could be investigated and selected as the optimum value for performing the experiments.
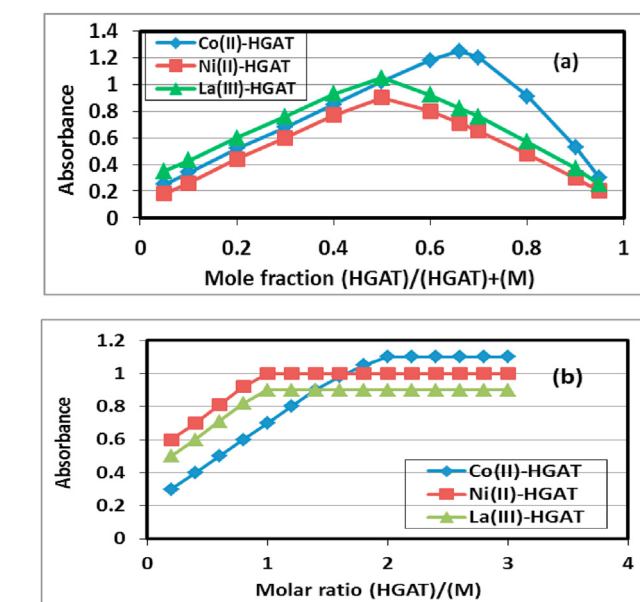
3.3. Effect of time

The effect of time on the absorption of HGAT-metal ions interaction was investigated to determine the time undertaking for complex formation. Study the effect of time was investigated at different time intervals up to one hour and represented graphically in Figure 4. The results indicated that the complex formation of Co(II) - [HGAT] interaction was the faster one and completed during 15 min while the complex formation for both Ni(II) - [HGAT] and La(III) - [HGAT] interaction was completed during 20 and 25 min, respectively.

3.4. Stoichiometry of the complexes

As clear from the experimental part, Job's continuous variation method and the molar ratio method, Figure 5 (a,b) were used to determine the stoichiometry of the complexes (Metal: HGAT ratio) existing in solution. Analysis of the obtained date from Figure 5a, it is clear that: The plot consists of two straight lines and offered maximum absorbance at mole fraction;

[HGAT]/[(M) + (HGAT)] = 0.672, 0.490 and 0.512 for Co(II), Ni (II) and La(III) ions, respectively indicating the stoichiometric composition of 1 : 2 (Metal: HGAT) for Co(II) ion while for Ni (II) and La(III) ions, the stoichiometric composition of 1 : 1 was achieved. This means that two molecules of HGAT could bind only one Co(II) ion while for Ni (II) and La(III) ions, one molecule of HGAT was involved under the stated experimental conditions. Additionally, as the mole fraction;
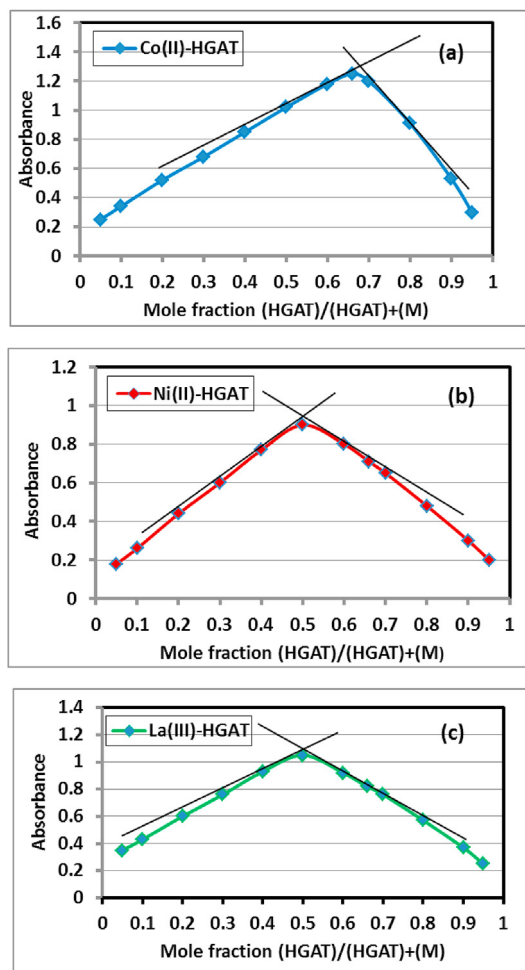

Figure 5. Different techniques applied to determine the stoichiometric ratio of HGAT – metal ions interaction in solution: (a) Job's continous variation method and (b) Molar ratio method.

Figure 6. The determination of stoichiometry of HGAT – metal ions interaction in solution by Job's method: (a) Co(II)-HGAT interaction, (b) Ni(II)- HGAT interaction and (c) La(III)-HGAT interaction.
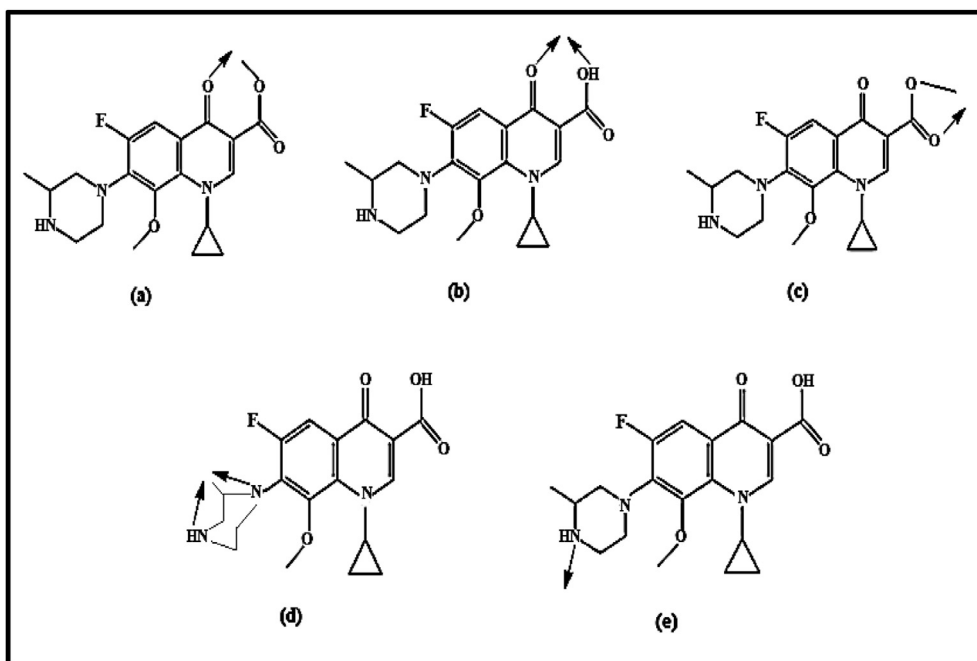
Figure 7. Possible coordination modes of HGAT towards the metal ions: (a–d) bidentate and (e) monodentate.

[HGAT]/[(M) + (HGAT)] increases from 0 to 1, the absorbance of the solution system under study increases firstly and decreases afterward and so, the number of molecules of HGAT per cation present in the complex (n) was determined through the relation; $n = x/(1-x)$ where; x is the mole fraction [29]. Moreover, the obtained date from Figure 5b displays the same metal ion to HGAT ratio. The molar ratio plots show an inflection with maximum absorbance at a molar ratio of [HGAT]/[M] = 2 for Co(II) ion while for Ni (II) and La(III) ions the observed inflection = 1.

3.5. Estimation the stability constant of HGAT-metal ions interactions

Estimation of the stability constants of the metal complexes resulted from the interactions between HGAT and Co(II), Ni(II) and La(III) ions in solution was an important aim of our work to provide an indication about the coordination behavior and the binding strength of HGAT drug towards the selected metal ions. The spectrophotometric measurements using Job's continuous variation method were used to estimate the formation constants of the metal complexes formed in solution as explained in Figure 6 (a-c) for Co(II), Ni(II), and La(III) ions, respectively [30]. Based on the obtained results, a simple equilibrium model between HGAT and the selected metal ions for the metal complexes formation can

Figure 8. The calibration plots of stoichiometry of HGAT – metal ions interaction in solution.

be represented as: $M + HGAT \rightleftharpoons [M(HGAT)]$ for 1:1 stoichiometry {M was Ni(II) or La(III) ion} while $M + 2HGAT \rightleftharpoons M(HGAT)_2]$ for the stoichiometry 1:2; where M was Co(II) ion. Additionally, the complex formation constant (K_f) can be evaluated using the mathematical relationship given as: $Kf = (A/A_m)/[1- (A/A_m)]^2C$ for 1:1 stoichiometry and $Kf = (A/A_m)/4C^2[1- (A/A_m)]^3$ for 1:2 stoichiometry, where; A is the observed maximum absorbance, A_m is the absorbance obtained from the extrapolation of the two lines obtained from Job's continuous variation curve and C is the initial molar concentration of study metal ion [31, 32]. Moreover, using the relationship; $\Delta G = - RTlnK$; Gibbs free energy (ΔG, kJ mol^{-1}) of the metal complexes formation can be estimated where, R is the gas constant (equal to 8.314 J mol^{-1} K^{-1}), T is the temperature in Kelvin and K is the determined stability constant [33].

The obtained values of K_f for the interaction of HGAT with Co(II), Ni(II) and La(III) ions were found to be 3.04×10^9, 4.73×10^4 and 4.67×10^4, respectively. It is clear that Co(II)- [HGAT] interaction has the higher stability formation constant value in comparison to Ni(II) - [HGAT] and La(III) - [HGAT] interaction. Additionally, the obtained negative values of ΔG for the same system; -5.41×10^4, -2.665×10^4 and -2.664×10^4, respectively. These negative values of ΔG mean that the kinetic process is a spontaneous one [34].

3.6. The suggested metal complexes structure

From a structural point of view and as clear from Figure 1, HGAT has variable functional groups at different positions as carboxylate, ketone and methoxy groups; piperazinyl and cyclopropyl moieties and a fluorine atom. The presence of these functional groups makes HGAT acts as an organic ligand with multi donor sites and has the ability to bind the metal ions with different manner forming variable metal complexes with a specific geometry [35]. Based on collective observations for several studies concerned with synthesis and characterization of metal complexes of HGAT, the possible coordination modes of HGAT are the carboxylato oxygen atom, pyridone oxygen atom and the piperazinyl ring nitrogen atom. Additionally, HGAT capable of bonding to the metal ion in a number of ways [36, 37, 38]. Figure 7 (a-e) shows the possible coordination modes of HGAT as:

Table 4. Optical characteristics and statistical data of the proposed method for interaction of HGAT drug with Co(II), Ni(II) and La(III) ions.

Parameters[a]	Analytical data[b]		
	Co(II)-HGAT	Ni(II)-HGAT	La(III)-HGAT
λ_{max} (nm)	500	650	340
Molar absorpitivity; ε (L mol^{-1} cm^{-1})	4.93×10^3	3.68×10^3	8.60×10^3
Beer's law limit (μg mL^{-1})	18.77–150.16	18.77–131.39	18.77–112.62
Sandell's sensitivity; SS (μg/cm^2/0.001 abs. unit)	0.077	0.103	0.044
Intercept (a)	0.1425	0.0871	0.2273
Slope (b)	0.0107	0.0081	0.0180
Correlation coefficient (r)	0.9982	0.9969	0.9998
Standard deviation SD	0.00732	0.005954	0.00649
Limit of detection; LOD (μg mL^{-1})	2.05	2.21	1.08
Limit of quantification; LOQ (μg mL^{-1})	6.84	7.35	3.61
Relative standard deviation; RSD (%)	0.955	1.144	0.560
Standard error; SE	0.001464	0.0011908	0.001298
Percentage error; % Error	0.139	0.170	0.092

[a] Number of standard sample for each metal ion - drug interaction under study was 8 and each one was repeated 5 times.
[b] The average of five replicates.

◆ A bidentate manner through:
   i. One of the oxygen atoms of deprotonated (undeprotonated) carboxylic group and the ring carbonyl oxygen atom (Figure 7a,b).
   ii. The two carboxyl oxygen atoms (Figure 7c).
   iii. Both piperazinic nitrogen atoms (Figure 7d).
◆ A monodentate manner through the terminal piperazinyl nitrogen (Figure 7e).

3.7. Method validation

Under the described experimental conditions, the calibration graph, Figure 8 was obtained by plotting the measured absorbance at the specified λ_{max} as a function of a varying concentration of HGAT. Each point of the calibration curve corresponding to the mean value obtained from eight independent measurements. The results showed that a linear relationships were obtained over the working concentration ranges of 18.77–150.16, 18.77–131.39 and 18.77–112.62 μg mL^{-1} for Co(II)-HGAT, Ni(II)-HGAT and La(III)-HGAT interaction at λmax 500, 650 and 340 nm respectively with good regression coefficient values of 0.9969–0.9998. Moreover, the high regression coefficients indicate the adherence of the calibration curves to Beer's law. Furthermore, the graph is described by the regression equation; $y = a + bx$ where; y is the absorbance, a is the intercept, b is the slope and x is the concentration of HGAT in μg mL^{-1} [39]. The calibration parameters including the slope, intercept and correlation coefficient are summarized in Table 4.

The limits of detection (LOD; the lowest amount of an analyte in a sample that can be detected by an analytical method) and limits of quantification (LOQ; the lowest amount of an analyte in a sample that can be quantitatively determined with acceptable accuracy) were calculated by using the following equations:

$$LOD = (3SD) / b$$

$$LOQ = (10SD) / b$$

$$SD = [\sum(X_i - \ddot{X})^2 / (N-1)]^{1/2}$$

where; *SD* is the standard deviation of the absorbance measurements, *b* is the slope of the calibration curve, X_i is the absorbance, $\ddot{X}$ is the mean value of X_i and N is the number of runs [40, 41, 42]. Additionally, the relative standard deviation (RSD %), standard error (SE) and the percentage error (% Error) were calculated from the relations given as [43, 44];

$$RSD = 100 \ (SD / \ddot{X}),$$

$$SE = SD / \sqrt{N}$$

$$\% \ Error = 100 \ (SE / \ddot{X})$$

The obtained LOD and LOQ values are shown in Table 4, confirming the sensitivity of the proposed technique. Also, the lower value of RSD (%) (1.144–0.560) and % Error (0.170–0.092) indicate the high accuracy of the methods.

3.8. Application of the proposed method

Under the worked experimental conditions, the designated method was performed to determine HGAT in its ophthalmic formulations as Tymer. All obtained results were tabulated in Table 5. It is worth noticing that, the results of the proposed method reveals a high level of accuracy where the % recovery was found to be 100.829 with a percentage error 0.276 and standard deviation 0.01088. This method characterized with its simplicity, easy to perform, carried out at room temperature, rapid, cheap and does not require special treatment of the sample under study.

3.9. Comparison with reported methods

Comparing the results of the present method with other reported methods [45, 46, 47] reveals that the present method could be applied successfully for the determination of HGAT in its pure bulk powder as well as its ophthalmic formulation.

Table 5. Comparison of the present method with reported method for the determination of HGAT in pharmaceutical formulation.

Parameters	Present method	Reported methods		
		Reference [45]	Reference [46]	Reference [47]
Recovery%	100.829	99.996	99.97	99.51
Sandell's sensitivity; SS (μg/cm^2/0.001 abs. unit)	0.074	0.493	0.040	0.470

4. Conclusions

The main focus of the presented work was on the development, optimize and validation of a spectrophotometric method for determination of gatifloxacin in pure form and in pharmaceutical formulation. Upon comparison of the suggested method with other reported methods, the former has the advantage of being simple which do not require complicated pretreatment of the sample, accurate and sensitive enough to enable determination of a lower amount of the drug and so, it is suitable for the determination of the studied drug in bulk and the pharmaceutical dosage forms.

Declarations

Author contribution statement

Mona M. Mostafa: Performed the experiments; Analyzed and interpreted the data.

Zeinab H. Abd El-Wahab: Conceived and designed the experiments; Analyzed and interpreted the data; Wrote the paper.

Aida A. Salman: Analyzed and interpreted the data; Wrote the paper.

W. M. Abdelbaset: Analyzed and interpreted the data; Contributed reagents, materials, analysis tools or data; Wrote the paper.

Funding statement

This research did not receive any specific grant from funding agencies in the public, commercial, or not-for-profit sectors.

Data availability statement

Data will be made available on request.

Declaration of interests statement

The authors declare no conflict of interest.

Additional information

No additional information is available for this paper.

References

[1] M.N. Saad, H.M. Essam, E.S. Elzanfaly, S.M. Amer, Economic chromatographic methods for simultaneous quantitation of some fluoroquinolones and corticosteroids present in different binary ophthalmic formulations, J. Liq. Chromatogr. Relat. Technol. 43 (2020) 271–281.
[2] M. Caianelo, C.R. Silva, M.G. Maniero, J.R. Guimaraes, Antimicrobial activity against Gram-positive and Gram-negative bacteria during gatifloxacin degradation by hydroxyl radicals, Environ. Sci. Pollut. Res. 24 (2017) 6288–6298.
[3] F.M.M. Salama, K.A.M. Attia, R.A.M. Said, M.M. Abdul-Aziz, M. El-Attar, First derivative synchronous fluorescence spectroscopy for the determination of Gatifloxacin in presence of its oxidative degradation product: Application to pharmaceutical preparation, Spectrochim. Acta Part A: Mol. Biomol. Spectrosc. 206 (2019) 302–313.
[4] R.A. Sversut, I.C. Alcantara, A.M. Rosa, A.C.M. Baroni, P.O. Rodrigues, A.K. Singh, M.S. Amaral, N.M. Kassab, Simultaneous determination of gatifloxacin and prednisolone acetate in ophthalmic formulation using first-order UV derivative spectroscopy, Arabian J. Chem. 10 (2017) 604–610.
[5] M.R. Siddiqui, Z.A. AlOthman, N. Rahman, Analytical techniques in pharmaceutical analysis: A review, Arabian J. Chem. 10 (2017) S1409–S1421.
[6] F. Zhang, S. Gu, Y. Ding, L. Li, X. Liu, Simultaneous determination of ofloxacin and gatifloxacin on cysteic acid modified electrode in the presence of sodium dodecyl benzene sulfonate, Bioelectrochemistry 89 (2013) 42–49.
[7] J. Sousa, G. Alves, A. Fortuna, A. Falcao, Analytical methods for determination of new fluoroquinolones in biological matrices and pharmaceutical formulations by liquid chromatography: a review, Anal. Bioanal. Chem. 403 (2012) 93–129.
[8] M.S. Attia, A.A. Essawy, A.O. Youssef, Europium-sensitized and simultaneous pH-assisted spectrofluorimetric assessment of ciprofloxacin, norfloxacin and gatifloxacin in pharmaceutical and serum samples, J. Photochem. Photobiol. A: Chem. 236 (2012) 26–34.
[9] I.A. Darwish, M.A. Sultan, H.A. Al-Arfaj, Selective kinetic spectrophotometric method for determination of gatifloxacin based on formation of its N-vinyl chlorobenzoquinone derivative, Spectrochim. Acta Part A: Mol. Biomol. Spectrosc. 75 (2010) 334–339.
[10] S.M. Al-Ghannam, Atomic absorption spectroscopic, conductometric and colorimetric methods for determination of some fluoroquinolone antibacterials using ammonium reineckate, Spectrochim. Acta Part A: Mol. Biomol. Spectrosc. 69 (2008) 1188–1194.
[11] H.M. Lotfy, D.A. Ahmed b, M.K. Abdel Rahman, S.A.F. Weshahy, Study of efficiency and spectral resolution for mathematical filtration technique using novel unlimited derivative ratio and classical univariate spectrophotometric methods for the multicomponent determination-stability analysis, Heliyon 5 (2019), e01669.
[12] A. Jouybana, E. Rahimpoura, Optical sensors based on silver nanoparticles for determination of pharmaceuticals: An overview of advances in the last decade, Talanta 217 (2020) 121071.
[13] M.F. Nazar, W. Azeem, A. Kayani, M. Zubair, P. John, A. Mahmood, M. Ashfaq, M.N. Zafar, S.H. Sumrra, M.N. Zafar, pH-dependent antibiotic gatifloxacin interacting with cationic surfactant: insights from spectroscopic and chromatographic measurements, J. Solut. Chem. 48 (2019) 936–948.
[14] M.A. Zayed, H.A. Dakhly, Spectrophotometric determination of gemifloxacin mesylate, moxifloxacin.HCl and gatifloxacin sesquihydrate in pure and in pharmaceutical preparations, Egypt. J. Chem. 58 (2015) 349–364.
[15] A.S. Amina, A.A. Goudab, R. El-Sheikh, F. Zahran, Spectrophotometric determination of gatifloxacin in pure form and in pharmaceutical formulation, Spectrochim. Acta Part A: Mol. Biomol. Spectrosc. 67 (2007) 1306–1312.
[16] F.A. Siddiqui, M.S. Arayne, N. Sultana, A.Z. Mirza, F. Qureshi, M.H. Zuberi, Facile and manifest spectrophotometric methods for the determination of six quinolone antibiotics in pharmaceutical formulations using iron salts, Med. Chem. Res. 19 (2010) 1259–1272.
[17] B. Cen, Y.X. Duan, L.Q. Deng, Y.L. Wang, X. Tao, Y.Z. Shen, Synthesis and structure characterization of homoleptic lanthanide complexes stabilized by Schiff-base ligands and their application in the polymerization of ε-caprolactone, J. Organomet. Chem. 857 (2018) 191–199.
[18] Z. Yaqin, Y. Binsheng, Spectral studies on the interaction between lanthanum ion and the ligand: N,N_-ethylenebis-[2-(o-hydroxyphenolic)glycine], Spectrochim. Acta, Part A 62 (2005) 641–644.
[19] M.R. Moghadam, S.M.P. Jahromi, A. Darehkordi, Analytical Methods, Simultaneous spectrophotometric determination of copper, cobalt, nickel and iron in foodstuffs and vegetables with a new bis thiosemicarbazone ligand using chemometric approaches, Food Chem. 192 (2016) 424–431.
[20] A.A. El-Asmy, T.H. Rakha, M.H. Abdel-Rhman, M.M. Hassanien, A.S. Al-Mola, Synthesis, spectral, thermal and biological studies on N-(2,4-dinitrophenyl)-2-mercaptoacetohydrazide and its metal complexes, Spectrochim. Acta Part A: Mol. Biomol. Spectrosc. 136 (2015) 1718–1727.
[21] O.A. Adegoke, O.E. Thomas, S.N. Emmanuel, Colorimetric determination of olanzapine via charge-transfercomplexation with chloranilic acid, J. Tabah Univ. Sci. 10 (2016) 651–663.
[22] F.A. Ibrahim, N.M. El-Enany, R.N. El-Shaheny, I.E. Mikhail, Spectroscopic studies on naftazone and its metal complexes with analytical applications for quality control of tablets, Anal. Methods 7 (2015) 5954–5961.
[23] A.S. Al-Kady, Optimized and validated spectrophotometric methods for the determination of trace amounts of uranium and thorium using 4-chloro-N-(2,6-dimethylphenyl)-2-hydroxy-5-sulfamoylbenzamide, Sens. Actuators, B 166–167 (2012) 485–491.
[24] F.A. Bernal, L.L.O. Diaz, E.C. Barrera, Exploitation of the complexation reaction of ortho-dihydroxylated anthocyanins with aluminum(III) for their quantitative spectrophotometric determination in edible sources, Food Chem. 185 (2015) 84–89.
[25] M.T. Alghamdi, A.A. Alsibaai, M.S. El-Shahawi, M.S. Refat, Structural and chelation behaviors of new Ru(II), Pt(IV) and Ir(III) gatifloxacin drug complexes: Spectroscopic characterizations, J. Mol. Struct. 1130 (2017) 264–275.
[26] F.A. Al-Saif, K.A. Alibrahima, J.A. Alfurhood, M.S. Refat, Synthesis, spectroscopic, thermal, biological, morphological and molecular docking studies of the different quinolone drugs and their cobalt(II) complexes, J. Mol. Liq. 249 (2018) 438–453.
[27] S.A. Sadeek, W.H. El-Shwiniy, Metal complexes of the fourth generation quinolone antimicrobial drug gatifloxacin: Synthesis, structure and biological evaluation, J. Mol. Struct. 977 (2010) 243–253.
[28] A.A. Akinsiku, O.O. Ajani, J.A. Adekoya, M.E. Emetere, E.O. Dare, Green synthesis of triclinic (anorthic) phase AgCoPO4 nanoparticles: optical studies and theoretical modelling, Heliyon 6 (2020), e05029.
[29] M.A.A. Islam, M.C. Sheikh, M. Abdul Mumit, R. Miyatake, M.A. Alam, M.O.A. Mondal, Synthesis, characterization and antimicrobial activity of a bidentate NS Schiff base of S-benzyl dithiocarbazate and its divalent complexes, J. Coord. Chem. 69 (2016) 3580–3592.
[30] L.H. Abdel-Rahman, A.M. Abu-Dief, A.A.H. Abdel-Mawgoud, Development, structural investigation, DNA binding, antimicrobial screening and anticancer activities of two novel quari-dentate VO(II) and Mn (II) mononuclear complexes, J. King Saud Univ. Sci. 31 (2019) 52–60.
[31] N.A. Annan, I.S. Butler, H.M. Titi, Y. El-Lazeik, B.J.J. Claude, S.I. Mostafa, DNA interaction and anticancer evaluation of new zinc(II), ruthenium(II), rhodium(III), palladium(II), silver(I) and platinum(II) complexes based on kojic acid; X-ray crystal structure of [Ag(ka)(PPh3)].H2O, Inorg. Chim. Acta. 487 (2019) 433–447.
[32] L.H. Abdel-Rahman, A.M. Abu-Dief, E.F. Newair, S.K. Hamdan, Some new nano-sized Cr(III), Fe(II), Co(II), and Ni(II) complexes incorporating 2-((E)-(pyridine-2-ylimino)methyl)napthalen-1-ol ligand: Structural characterization, electrochemical, antioxidant, antimicrobial, antiviral assessment and DNA interaction, J. Photochem. Photobiol. B Biol. 160 (2016) 18–31.
[33] M.K. Saroj, R. Payal, S.K. Jain, N. Sharma, R.C. Rastogi, Investigation of indole chalcones encapsulation in β-cyclodextrin: determination of stoichiometry, binding

constants and thermodynamic parameters, J. Incl. Phenom. Macro. Chem. 90 (2018) 305–320.

[34] O. Altun, M. Suozer, Synthesis, spectral analysis, stability constants, antioxidant and biological activities of Co (II), Ni (II) and Cu (II) mixed ligand complexes of nicotinamide, theophylline and thiocyanate, J. Mol. Struct. 1149 (2017) 307–314.

[35] Z. Xu, S.J. Zhao, Z.S. Lv, F. Gao, Y. Wang, F. Zhang, L. Bai, J.L. Deng, Fluoroquinolone-isatin hybrids and their biological activities, Eur. J. Med. Chem. 162 (2019) 396–406.

[36] K. Althubeiti, In binary solvent: Synthesis and physicochemical studies on the nanometric palladium(II) oxide associated from complexity of palladium(II) ions with gatifloxacin drug as a bio-precursors, J. Mol. Struct. 1205 (2020) 127604.

[37] F.A. Al-Saif, K.A. Alibrahim, J.A. Alfurhood, M.S. Refat, Synthesis, spectroscopic, thermal, biological, morphological and molecular docking studies of the different quinolone drugs and their cobalt(II) complexes, J. Mol. Liq. 249 (2018) 438–453.

[38] G. Hancu Rusu, A.C. Munteanu, V. Uivarosi, Development perspectives of silver complexes with antibacterial quinolones: Successful or not? J. Organomet. Chem. 839 (2017) 19–30.

[39] S.A. Errayess, A.A. Lahcen, L. Idrissi, C. Marcoaldi, S. Chiavarini, A. Amine, A sensitive method for the determination of Sulfonamides in seawater samples by Solid Phase Extraction and UV–Visible spectrophotometry, Spectrochim. Acta Part A: Mol. Biomol. Spectrosc. 181 (2017) 276–285.

[40] P.R.N. Bhuket, W. Wichitnithad, O. Sudtanon, P. Rojsitthisak, A stability-indicating UPLC method for the determination of curcumin diethyl disuccinate, an ester prodrug of curcumin, in raw materials, Heliyon 6 (2020), e04561.

[41] S.N.H. Azmi, B. Iqbal, N.S.H. Al-Humaimi, I.R.S. Al-Salmani, N.A.S. Al-Ghafri, N. Rahman, Quantitative analysis of cefixime via complexation with palladium(II) in pharmaceutical formulations by spectrophotometry, J. Pharm. Anal. 3 (2013) 248–256.

[42] G. Murtaza, Y. Akhtar, T. Mahmood, S.M.A. Abid, P. Makreski, A novel UV-spectrophotometric for simultaneous estimation of amlodipine and captopril, Pharm. Chem. J. 52 (2019) 952–958.

[43] F. Belal, M.A. Omar, S. Derayea, S. Zayed, M. Abdelkhalek Hammad, S.F. Saleh, Simultaneous determination of paracetamol, caffeine and codeine in tablets and human plasma by micellar liquid chromatography, Eur. J. Chem. 6 (2015) 468–474.

[44] M.F. Cheira, A.S. Orabi, M.A. Hassanin, S.M. Hassan, Solvent extraction of thorium (IV) from chloride solution using Schiffbase and its application for spectrophotometric determination, Chem. Data Collec. 13–14 (2018) 84–103.

[45] A.M. El-Didamony, M.O. Abo-Elsoad, Kinetic spectrophotometric method for the determination of some fourth generation fluoroquinolones in bulk and in pharmaceutical formulations, J. Saudi Chem. Soc. 21 (2017) S58–S66.

[46] I.A. Aljuffali, M. Abul Kalam, Y. Sultana, A. Imran, A. Alshamsan, Development and validation of stability-indicating high performance liquid chromatography method to analyze gatifloxacin in bulk drug and pharmaceutical preparations, Saudi Pharm. J. 23 (2015) 85–94.

[47] K. Venugopal, R.N. Saha, New, simple and validated UV-spectrophotometric methods for the estimation of gatifloxacin in bulk and formulations, Il Farmaco 60 (2005) 906–912.